JOURNAL OF GEOPHYSICAL RESEARCH, VOL. 96, NO. C8, PAGES 15,147–15,159, AUGUST 15, 1991

Basin-Scale Estimates of Oceanic Primary Production by Remote Sensing: The North Atlantic

TREVOR PLATT, CARLA CAVERHILL, AND SHUBHA SATHYENDRANATH[1]

Biological Oceanography Division, Bedford Institute of Oceanography, Dartmouth, Nova Scotia, Canada

The estimation by remote sensing of annual primary production at ocean basin scales is illustrated for the Atlantic Ocean, using the monthly averaged Coastal Zone Color Scanner data for 1979. The principal supplementary data used were some 873 vertical profiles of chlorophyll and some 248 sets of parameters derived from photosynthesis-light experiments. This information was used to parametrize the local algorithm for calculation of primary production in 12 subregions of the entire domain for each of the four seasons. Four different procedures were tested for calculation of primary production. These differed according to whether the autotrophic biomass distribution was uniform with depth and whether the irradiance was resolved with respect to wavelength: the spectral model with nonuniform biomass was considered as the benchmark for comparison against the other three models. At particular locations and times, the less complete models gave results that differed by as much as 50% from the benchmark. After integration to basin scale, vertically uniform models tended to underestimate primary production by about 20% compared to the nonuniform models. At large horizontal scale, the differences between spectral and nonspectral models were negligible, a result that was believed to follow from mutual compensation of underestimates and overestimates, according to the local biomass, in different parts of the domain. Calculation of primary production is highly sensitive to the algorithm used to retrieve the biomass. The linear correlation between biomass and estimated production was poor outside the tropics, suggesting caution against the indiscriminate use of biomass as a proxy variable for primary production. The annual primary production for the Atlantic between 20°S and 70°N was 9 ± 3 Gt yr^{-1}, higher than previous estimates made without reference to remotely sensed data. It is argued that the remote-sensing method is the method of choice for calculation of primary production at the ocean basin scale.

INTRODUCTION

The advent of remotely sensed data on ocean color has made the synoptic estimation of primary production for entire ocean basins an attainable goal. Progress in this direction requires that we address two issues: choice of a local algorithm for primary production and its extrapolation to large spatial scales [*Platt and Sathyendranath*, 1988].

Selection of a model to parametrize the primary production at local scales of space and time involves a decision on how to handle nonuniformity in the vertical profile of phytoplankton pigments [*Platt et al.*, 1988]. A decision is also required on the level of complexity in the description: whether the model will include the wavelength and angular structure of the submarine light field [*Sathyendranath and Platt*, 1989*a*; *Sathyendranath et al.*, 1989], whether a linear model of the photosynthesis-light curve will suffice [*Platt*, 1986], and whether the parameters of the photosynthesis-light curve will be considered as local constants or allowed to vary with depth.

Extrapolation of the local algorithm to regional scales is a trivial problem if a minimalist parametrization is used, that is, one with a linear photosynthesis-light curve of universally constant slope [*Platt*, 1986] and insensitive to wavelength or angular structure of the light field and in which the concentration of photosynthetic pigments is assumed to be vertically homogeneous. Such a model, however, would be useful for only the crudest of estimates of primary production. In practice, some selection of parameters is required, either for the shape of the vertical pigment profile [*Platt et al.*, 1988] or the photosynthesis-light curve, or both. A parsimonious approach is to partition the ocean into a set of subregions within which the required parameters can be considered constant for a particular season [*Platt and Sathyendranath*, 1988; *Mueller and Lange*, 1989]. By analogy with the biogeographic provinces of taxonomical interest, these oceanic subregions might be called biogeochemical provinces.

In this paper we consider the problems outlined above in the context of estimating the primary production of the North Atlantic Ocean by remote sensing. We discuss the data available for the parametrization of the photosynthesis-light curve and for the vertical profile of photosynthetic pigments within different biogeochemical provinces and how the parameters vary with season. Given the parameter sets, we then compare four different protocols for computation of water column primary production (nonlinear models of differing complexity): spectrally neutral models with or without vertically homogeneous biomass and spectrally sensitive models with or without vertically homogeneous biomass. On the assumption that the most complex model (nonlinear, spectrally sensitive, photosynthesis-light curve; nonuniform biomass profile) gives the best estimate [*Platt and Sathyendranath*, 1988], the relative error of the other three protocols is calculated. Finally, the results are used to discuss the seasonal and regional distribution of primary production in the North Atlantic Ocean.

THE LOCAL ALGORITHMS

Our objective is to estimate water column primary production given remotely sensed data on ocean colour, which

[1]Also at Department of Oceanography, Dalhousie University, Halifax, Nova Scotia, Canada.

Paper number 91JC01118.
0148-0227/91/91JC-01118$05.00

are interpreted as surface concentrations of chlorophyll pigments. We consider four alternative protocols for the local algorithm, each of which is based on a nonlinear representation of the photosynthesis-light curve. The general procedure is to calculate primary production as a function of depth and integrate through the photic zone. Light available at the surface is obtained by calculation, assuming a cloud-free sky, and corrected for the effect of clouds using independent information. The production at any depth depends on the biomass at that depth and also, through its effect on the submarine light field, on the biomass at all shallower depths.

The alternative algorithms for estimating primary production differ in the way the parametrization is handled for the photosynthesis-light curve and for the biomass profile.

Biomass Profile

Let $B(z)$ be the photosynthetically active biomass at depth z. In principle, the remotely sensed estimates of chlorophyll refer to the surface biomass $B(0)$, but in practice, there is some contribution to the estimate from depths below the surface. We therefore define a satellite-weighted chlorophyll estimate B_s, the apparent surface chlorophyll concentration as seen by the satellite [*Gordon and Clark*, 1980]. For those local algorithms that assume vertically homogeneous biomass, the biomass is set equal to B_s at all depths.

The biomass profile $B(z)$ may be parametrized as follows [*Platt et al.*, 1988]:

$$B(z) = B_0 + \frac{h}{\sigma(2\pi)^{1/2}} \exp\left[-\frac{(z - z_m)^2}{2\sigma^2}\right] \tag{1}$$

where the background biomass B_0 has superimposed on it a Gaussian with parameters z_m, the depth of the chlorophyll maximum; σ, a measure of the thickness or vertical spread of the peak; and h, the total biomass in the peak such that h/σ is a measure of the height of the peak above background. Thus, in principle, four parameters should be assigned for a complete description of the pigment profile. Access to remotely sensed estimates of B_s, however, relaxes this requirement in that only three additional pieces of information need be supplied to characterize the profile [*Sathyendranath and Platt*, 1989*b*]. The reduction from 4 to 3 degrees of freedom is accomplished through definition of the dimensionless quantity ρ equal to the ratio of the peak biomass to the background biomass:

$$\rho = h/[B_0\sigma(2\pi)^{1/2}]. \tag{2}$$

For those local algorithms in which the biomass is allowed to vary with depth, the shape of the biomass profile is described by the set of parameters z_m, ρ, and σ, while the scale factor, given by $\{B_0 + h/[\sigma(2\pi)^{1/2}]\}$, is specified by information from the satellite. The procedure used to recover equation (1) is given by *Sathyendranath and Platt* [1989*b*].

Photosynthesis-Light Curve

Let $I(z, \lambda)$ be the irradiance at depth z, where λ is the wavelength ($400 \le \lambda \le 700$ nm). Let $P(z)$ be the rate of primary production. For those local algorithms in which the wavelength and the angular structure of the light field are suppressed, the dependence of primary production on available light can be written [*Smith*, 1936; *Platt et al.*, 1988] as

$$P(z) = \frac{B(z)\alpha^B I(z)}{\{1 + [\alpha^B I(z)/P_m^B]^2\}^{1/2}} \tag{3}$$

where the biomass-specific parameters of the photosynthesis-light curve are α^B, the initial slope, and P_m^B, the assimilation number.

For those local algorithms in which the dependence on spectral and angular structure of the light field is retained, equation (3) can be rewritten [*Platt and Sathyendranath*, 1988; *Sathyendranath and Platt*, 1989*a*] as

$$P(z) = \frac{B(z)\Pi(z)}{\{1 + [\Pi(z)/P_m^B]^2\}^{1/2}} \tag{4}$$

where

$$\Pi(z) = \sec\theta \int \alpha^B(z, \lambda) I_d(z, \lambda; \theta)\, d\lambda + 1.2 \int \alpha^B(z, \lambda) I_s(z, \lambda)\, d\lambda \tag{5}$$

and where the irradiance I has been partitioned into two components, the direct sunlight I_d with in-water zenith angle θ and the diffuse sky light I_s. The shape of $\alpha^B(\lambda)$ is considered to be known [*Sathyendranath et al.*, 1989]: its scale is fixed such that the average over a neutrally white incident spectrum is equal to the α^B of equation (3).

Irradiance at the Sea Surface

The incident irradiance field, $I_d(0, \lambda)$ and $I_s(0, \lambda)$, is constructed, initially assuming a cloud-free sky, using the model of *Bird* [1984] as applied by *Sathyendranath and Platt* [1988]. The approach to a correction for cloud cover is as follows: Total shortwave radiation at the ground, in the presence of clouds, I_T, is given by [*Paltridge and Platt*, 1976]

$$I_T(\theta') = I_{\text{ext}}\left(1 - \sum_i A_{ci}F_i\right)[1 - \hat{m} - A_a(1 - F)] \cos\theta' \tag{6}$$

where I_{ext} is the (extraterrestrial) solar constant, A_{ci} is the albedo of clouds at level i and the atmosphere above it, F_i is the fractional cloud cover at level i, $\hat{m}$ is absorption by water vapor, A_a is the albedo of the atmosphere in the clear-sky fraction, F is total cloud cover (expressed as a fraction), and θ' is the Sun zenith angle (in air).

According to *Paltridge and Platt* [1976], the cloud albedo varies from 0.35 to 0.60 depending on cloud type. Here, we assume access to data on cloud cover but not on cloud type and therefore assign a mean value of 0.5 for cloud albedo and replace ΣF_i by F, the total cloud cover. *Paltridge and Platt* [1976] have also noted that absorption by water vapor saturates at about 0.18, with no additional absorption in the presence of clouds, and that is the value we have adopted for $\hat{m}$. Atmospheric albedo A_a is computed assuming a Rayleigh atmosphere [*Paltridge and Platt*, 1976]:

$$A_a = 0.28/(1 + 6.43 \cos\theta'). \tag{7}$$

By substituting $F = 0$ in (6), one can compute $I_T(\theta')$ in the absence of clouds. The fractional decrease R in total shortwave radiation at the ground due to clouds is then given by

$$R = \frac{(1 - 0.5F)[1 - \hat{m} - A_a(1 - F)]}{[1 - \hat{m} - A_a]}. \quad (8)$$

The effect of clouds includes a decrease in direct irradiance as well as a possible increase in diffuse light due to cloud scattering. The fractional decrease R_d in direct light is estimated as

$$R_d = (1 - F). \quad (9)$$

Now, let I_d^{clear}, I_s^{clear} and I_t^{clear} be the integrals over wavelength of direct, sky, and total irradiance at the ground, for the photosynthetically active region (400–700 nm), as computed from the clear sky model ($I_t^{clear} = I_d^{clear} + I_s^{clear}$). Then, the diffuse irradiance at sea level in the presence of clouds is given by

$$I_s = I_t^{clear}R - I_d^{clear}R_d, \quad (10)$$

and the fractional change in diffuse light is computed as

$$R_s = I_s/I_s^{clear}. \quad (11)$$

Finally, the spectral values of I_d^{clear} and I_s^{clear} are multiplied by R_d and R_s, respectively. Note that this approach applies a crude correction for the change in total irradiance at sea level and for the change in the proportions of direct and sky light but makes no concession for any possible spectral effects on the diffuse component.

Submarine Light Field

For the nonspectral models, the submarine light field $I(z)$ was calculated from the following equation [*Sathyendranath and Platt*, 1988]:

$$I(z) = I_0 \exp\left[-\int_s (K_w + C(z')k_c)\, dz'\right], \quad (12)$$

where I_0 is the irradiance just below the surface; $C(z)$ is the concentration of all phytoplankton pigments, both photosynthetically active and detrital; K_w is the attenuation coefficient for pure seawater; and k_c is the specific absorption coefficient for phytoplankton. Attenuation coefficient due to any material, particulate or dissolved, uncorrelated with chlorophyll, is assumed to be zero. The coefficient k_c includes the effect of yellow substances, assumed to covary with phytoplankton.

In the case of the spectral models, the direct and diffuse components of irradiance are handled separately, with vertical attenuation coefficients K_d and K_s, respectively, given by [*Sathyendranath and Platt*, 1988]

$$K_d(z, \lambda) = [a(z, \lambda) + b_b(z, \lambda)]/\cos\theta, \quad (13)$$

and

$$K_s(z, \lambda) = [a(z, \lambda) + b_b(z, \lambda)]/0.83, \quad (14)$$

where $a(z, \lambda)$ is the total volume absorption coefficient of the water, $b_b(z, \lambda)$ is the backscattering coefficient, and 0.83 (inverse of 1.2, cf. equation (5)) is the mean cosine for uniformly diffuse light assuming refraction at a flat sea surface [*Sathyendranath and Platt*, 1989*a*].

TABLE 1. Subdivision of the Study Domain Into Regions Based on Latitude and the Depth of the Water Column

Depth Range			
Shelf (<200 m)	Slope	Deep (>2000 m)	Latitude Range
1	5	9	subarctic (51°N to 70°N)
2	6	10	transitional (38°N to 50°N)
3	7	11	subtropical (11°N to 37°N)
4	8	12	equatorial (10°S to 10°N)
3	7	11	subtropical (20°S to 11°S)

Note that the subtropical regions are assigned the same number on both sides of the equator.

Algorithm Alternatives

We considered four alternative algorithms for the estimation of local, water column primary production. Each uses the same basic, nonlinear form of the photosynthesis-light curve. In order of increasing complexity they are model 1, nonspectral model with homogeneous biomass profile; model 2, nonspectral model with inhomogeneous biomass profile; model 3, spectral model with homogeneous biomass profile; and model 4, spectral model with inhomogeneous biomass profile, where "homogeneous" means uniform with depth and of magnitude equal to the satellite-derived concentration B_s.

An essential first step for implementation of the algorithms is selection of the parameters for the biomass profile and the photosynthesis-light curve. This is the subject of the next section.

PARAMETER SELECTION

Our general approach to parameter selection was first to subdivide the North Atlantic into (12) subregions with respect to latitude and bathymetry. The latitudinal zones are equatorial (10°S to 10°N); subtropical (11°S to 20°S and 11°N to 37°N); transitional (38°N to 50°N); and subarctic (51°N to 70°N). The three categories of depth were shelf (less than 200 m); slope (from 200 to 2000 m); and deep (greater than 2000 m). The 12 subregions that result from this four-by-three classification (Table 1) represent a preliminary step toward the delineation of biogeochemical provinces in the North Atlantic. Data archives were searched for relevant information, which was sorted by season according to the following scheme: winter (December to February); spring (March to May); summer (June to August); and fall (September to November).

Biomass Profile

Some 873 chlorophyll profiles were obtained from 25 bibliographic sources (Table 2*a*). The profiles were fitted to equation (1) for parameter estimation. Initially, only those profiles with 10 or more depths were considered acceptable, giving at least 6 degrees of freedom in the residual variance for the four-parameter fit. However, in some cases a given subregion in a given season might have only profiles with fewer than 10 data points, and in these cases, profiles with as few as six data points were admitted. These were found to be

TABLE 2*a*. Sources of Data for Chlorophyll Profile Parameterization

Source	Area of Study	Year	Number of Profiles
Bermuda Biological Station [1960] and *Woods Hole Oceanographic Institution* [1964]	Station S (off Bermuda)	1957–1963	38 (56)
Biological Oceanography Division Bedford Institute of Oceanography (unpublished data, 1990)	a, Caribbean	1984	20 (23)
	b, Labrador Sea	1984	14 (16)
	c, Georges Bank	1985	5 (11)
	d, Sargasso Sea	1985	1 (2)
Denman et al. [1977]	Scotian Shelf	1976	62 (65)
A. Herbland (personal communication, 1990)	Equatorial Atlantic	1979	82 (91)
Irwin and Platt [1979]	Scotian Shelf	1978	22 (23)
Irwin et al. [1978*c*]	Scotian Shelf	1977	26 (26)
Irwin et al. [1978*d*]	Baffin Bay	1977	3 (3)
Irwin et al. [1983*c*]	Foxe Basin	1981	4 (9)
Irwin et al. [1983*d*]	Scotian Shelf	1979	5 (14)
Irwin et al. [1983*e*]	Azores	1981	10 (10)
Irwin et al. [1985*a*]	Sargasso Sea	1983	28 (28)
Irwin et al. [1985*b*]	Eastern Arctic	1983	8 (9)
Irwin et al. [1986*a*]	Labrador Sea	1984	9 (15)
Irwin et al. [1986*b*]	Grand Banks	1984	1 (4)
Irwin et al. [1987*a*]	a, Georges Bank	1985	4 (70)
	b, Sargasso Sea		0 (2)
Irwin et al. [1987*b*]	Caribbean	1984	13 (19)
Irwin et al. [1988*b*]	Celtic Sea	1986	37 (40)
Irwin et al. [1988*c*]	Hudson Bay	1982	4 (9)
Irwin et al. [1988*d*]	Grand Banks	1985	14 (16)
Irwin et al. [1989*a*]	New England Seamounts	1987	103 (112)
Irwin et al. [1990*a*]	Sargasso Sea	1988	15 (15)
Irwin et al. [1990*b*]	Georges Bank	1988	4 (25)
Irwin et al. [1990*c*]	Labrador Sea	1988	17 (17)
Irwin et al. [1991]	North Atlantic	1989	30 (31)
J. E. O'Reilly (personal communication, 1990) *O'Reilly and Busch* [1984] and *O'Reilly et al.* [1987]	NW Atlantic shelf	1979	42 (112)
	Total		621 (873)

The number of profiles that could be used for curve fitting is given in the last column: the number in parentheses indicates the total number of profiles that was available.

adequate to characterize the profile, provided that the data points were well distributed around the peak.

Some 145 profiles had an unfortunate distribution of sampling depths (missing values near the surface, ill-defined peak, or profiles that did not extend deep enough to resolve the peak) and were therefore not used in the analysis. Profiles were also discarded for other reasons: Six profiles showed more than one chlorophyll peak and were discarded as being incompatible with equation (1). We were unable to find satisfactory parameter estimates in the case of 10 profiles (this problem usually occurred when the chlorophyll values decreased in an exponential fashion from the surface, which made it impossible to fix z_m and σ). Some 91 profiles were from the Georges Bank region: we considered that data from this tidal front area should not be used to characterize large-scale features as attempted here, and these profiles were therefore discarded. After the results were grouped by region and season, 12 profiles differing markedly from others in the same subset were also discarded.

Finally, some 609 of the initial 873 profiles were considered usable for parameter selection. These profiles were not distributed uniformly in space and time. The distribution ranged from 110 profiles for region 11 in summer, to none in 20 of the 48 zones (12 regions and four seasons). The mean parameters for each region and season were then calculated, where data were available. For seven zones, the "typical" profiles are based on single profiles.

For temperate and subarctic regions in winter, no data were available, and in these instances, we assumed uniform profiles for the biomass. This assumption was made on the grounds that winter mixing and buoyancy forcing, and consequent deepening of the mixed layer, would render uniform profiles the norm rather than the exception. We also computed the photic depth for these regions in winter, with the satellite-derived biomass data and the light transmission model of *Sathyendranath and Platt* [1988] and found that the computed photic depths were generally less than the depths of the mixed layer reported for these regions [*Levitus*, 1982].

For the remaining regions and seasons where data were unavailable, the parameters from adjacent blocks were used. The entire parameter set, for each region and season, as used in the calculations that follow, is given in Table 3. The generalized profiles corresponding to these parameters are shown in Figure 1.

Light Saturation Curve

The parameters for the light saturation curve (initial slope α^B and assimilation number P_m^B) were all taken from cruises of the Biological Oceanography Division of the Bedford Institute of Oceanography (sources in Table 2*b*). In these cruises, photosynthesis-light experiments are made routinely in incubators on the ship. The procedure for extraction of the photosynthesis parameters for these experiments and the underlying theory are given by *Platt et al.* [1980]. To avoid the possibility of including results for P_m^B based on

TABLE 2*b*. Sources of Data on Photosynthesis-Light Parameters for the North Atlantic Ocean

Source	Area of Study	Year	Number of Observations
Irwin et al. [1975]	a, St. Margaret's Bay	1973–1975	30
	b, Bedford Basin		18
	c, Chebucto Head		4
Denman et al. [1977]	Scotian Shelf	1976	15
Irwin and Platt [1979]	Scotian Shelf	1978	1
Irwin et al. [1978*a*]	Labrador Sea	1977	15
Irwin et al. [1978*b*]	Labrador Sea	1978	16
Irwin et al. [1978*d*]	Baffin Bay	1977	4
Irwin et al. [1980]	Scott Inlet	1978	5
Irwin et al. [1983*d*]	Scotian Shelf	1979	11
Irwin et al. [1982]	Ungava Bay	1979	2
Irwin et al. [1983*a*]	Azores	1982	4
Irwin et al. [1983*b*]	Eastern Arctic	1980	6
Irwin et al. [1983*c*]	Foxe Basin	1981	4
Irwin et al. [1983*e*]	Azores	1981	1
Irwin et al. [1985*a*]	Sargasso Sea	1983	1
Irwin et al. [1985*b*]	Eastern Arctic	1983	6
Irwin et al. [1986*a*]	Labrador Sea	1984	1
Irwin et al. [1986*b*]	Grand Banks	1984	1
Irwin et al. [1987*a*]	a, Georges Bank,	1985	22
	b, Sargasso Sea		2
Irwin et al. [1987*b*]	Caribbean	1984	10
Irwin et al. [1988*a*]	Bedford Basin	1985	23
Irwin et al. [1988*b*]	Celtic Sea	1986	4
Irwin et al. [1988*d*]	Grand Banks	1985	6
Irwin et al. [1989*a*]	New England Seamounts	1987	2
Irwin et al. [1989*b*]	Labrador Sea	1985	6
Irwin et al. [1990*a*]	Sargasso Sea	1988	3
Irwin et al. [1990*b*]	Georges Bank	1988	15
Irwin et al. [1990*c*]	Labrador Sea	1988	10
	Total		248

populations photoadapted to low light, only data from 10 m or shallower were admitted. The relevant data then consisted of some 248 light saturation experiments. The data were sorted by region and season, as for the biomass profiles. The entire parameter set, for each region and season, as used in the calculations that follow, is given in Table 4. The parameters were taken to be constant with depth.

Forcing Fields

The local algorithms are forced by the biomass and irradiance fields. The irradiance field is obtained by computation for a cloud-free sky and subsequently scaled for the effect of clouds.

Cloud Cover Field

Data on surface observations of global cloud cover were obtained from the archives of the National Center for Atmospheric Research, Boulder, Colorado [see *Hahn et al.*, 1987]. The relevant data on mean-monthly cloud cover for 1979 had a resolution of 5° (latitude) by 5° (longitude) for the region from 20°S to 50°N; and 5° (latitude) by 10° (longitude) for the region from 50°N to 70°N. The data were expressed as percent cloud cover. Where data were lacking for 1979, the long-term mean was used as a proxy (about 1% of cases) if available. If not, the mean of the surrounding blocks was used (about 2% of cases).

Biomass Field

We used the Coastal Zone Colour Scanner (CZCS) level 3 monthly-averaged fields of biomass for the North Atlantic in 1979, obtained from the National Aeronautics and Space Administration. We used these data, averaged on a 1° × 1° grid, to recalculate the corresponding blue-green ratios. The vertical biomass structure was then derived from the data, with the parameters of Table 3, using the procedure of *Sathyendranath and Platt* [1989*b*].

Results and Discussion

With the given forcing fields, each of the four local algorithms was applied for each of the 12 months of 1979 at each node of a 1° × 1° grid. Computations were carried out for the fifteenth day of every month, with results taken as representative for that month. The output for each algorithm was a series of vertical profiles of primary production (vertical resolution 1 m) calculated every half hour. Each profile was integrated over depth and the integrals summed through time to yield estimates of daily rates of water column production representative of the month in question. The set of daily integrals forms the raw material for the rest of the discussion in this paper.

Comparison Between Models

To compare the results of the four alternative algorithms, we computed the average production for each month, and

TABLE 3. Parameters of the Vertical Biomass Profile for the 12 Regions of the Atlantic in Four Seasons

Region	σ, m	z_m, m	ρ	N
		Winter		
1	*	*	*	0
2	*	*	*	0
3	56	41	—	1
4[a]				
5	*	*	*	0
6	*	*	*	0
7	36 (35)	38 (55)	0.94 (88)	5
8[b]				
9	*	*	*	0
10	*	*	*	0
11	47 (78)	50 (51)	10.3 (339)	38
12	11 (21)	47 (13)	7.19 (50)	10
		Spring		
1	16 (7)	10 (29)	50.1 (69)	6
2	14 (51)	15 (42)	51.5 (211)	41
3	13	−8	1.62	1
4[c]				
5	12 (54)	15 (89)	34.0 (86)	9
6	15 (45)	13 (62)	639 (334)	29
7[d]				
8[e]				
9[f]				
10	23 (27)	16 (46)	72.3 (151)	33
11	33 (55)	51 (60)	13.5 (261)	53
12[e]				
		Summer		
1	5 (30)	15 (43)	18.4 (158)	7
2	9 (54)	27 (32)	6.52 (65)	42
3	5	3	0.96	1
4[c]				
5	13 (62)	20 (132)	9.28 (88)	8
6	11 (53)	32 (30)	31.2 (264)	67
7[e]				
8[e]				
9	10 (64)	36 (23)	6.95 (125)	18
10	10 (56)	40 (31)	20.4 (176)	19
11	21 (32)	81 (17)	12.0 (85)	110
12[e]				
		Fall		
1	40 (2)	−20 (10)	5.70 (45)	2
2	6 (62)	28 (16)	4.00 (45)	12
3[g]				
4[h]				
5	20 (56)	24 (45)	7.5 (67)	3
6	4	18	17.9	1
7[i]				
8	7	48	5.03	1
9	4	23	29.1	1
10	7	29	31.0	1
11	17 (21)	84 (7)	4.11 (33)	19
12	15 (54)	49 (16)	3.22 (89)	71

For each parameter, the entry includes the mean over N observations, followed by the coefficient of variation (%) in parentheses. A dash in the ρ column means that B_0 is zero, and therefore ρ is indeterminate. Negative values of z_m indicate that the biomass peak is at the surface, with the imaginary maximum of the generalized profile located above the surface.

*Biomass profile is vertically uniform.

[a]No data: used region 3 (winter) data.

[b]No data: used region 12 (winter) data.

[c]No data: used region 3 (summer) data.

[d]No data: used region 11 (spring) data.

[e]No data: used region 11 (summer) data.

[f]No data: used region 5 (spring) data.

[g]No data: used region 2 (fall) data.

[h]No data: used region 8 (fall) data.

[i]No data: used region 11 (fall) data.

for each region. We found that the differences between the models were, on the whole, not negligible (Figure 2).

The differences in the estimates between models 1 and 2 and between models 3 and 4 are measures of the effect of ignoring the vertical structure of the water column in computation of primary production from remotely sensed data. The differences between the estimates from models 2 and 4 and models 1 and 3 are measures of the effect of ignoring the spectral structure of the light field in estimating primary production from remotely sensed data on ocean colour. However, it is not possible to separate entirely the effect of spectral structure from that of profile structure, since interactive effects between them undoubtedly occur. Note that the differences between models are due to systematic rather than random causes: it is therefore inappropriate to apply statistical procedures to them as tests of significance.

Model 4 (nonuniform, spectral version) is theoretically the most complete, and its applicability has already been demonstrated [*Platt and Sathyendranath*, 1988]. Therefore we used this model as the benchmark to evaluate the performance of the other three models. These comparisons showed that for a given month and region, the model 1 prediction could be as low as 38% of model 4 or as high as 121% of it. Similarly, model 2 sometimes severely underestimated production, when compared to model 4, but on other occasions it gave an overestimate (range from 48% to 136%). The relative magnitudes of primary production calculated for models 3 and 4 lay within a similar range.

It can be seen (Figure 2) that these differences vary between regions and seasons in a complex manner that suggests no obvious pattern. As shown by *Platt et al.* [1988] and *Sathyendranath et al.* [1989], these differences depend on the parameter values for photosynthesis and for the pigment profile, as well as on the driving force, the surface irradiance. Situations will occur, for favorable combinations of these parameters, when the models differ little from each other. Moreover, extreme conditions may arise in which the benchmark model is not necessarily the most reliable. An example of this is in region 1, summer, where the biomass values (as estimated by the algorithm of *Sathyendranath and Platt* [1989*b*]) far exceed the range for which the light transmission model was designed ($C \leq 10$ mg m^{-3}). In this case, the apparent, large difference between model 4 and the rest is misleading.

Since, for any one model, both positive and negative differences (relative to model 4) are observed in different subregions, averaging over the whole basin reduces some of the differences. When the integrals for the whole basin (20°S to 70°N) were compared, it was found that the results of vertically uniform models (models 1 and 3) differed from those of model 4 by only 20% or less for any month but that the uniform models generally underestimated production. In the presence of a surface bloom, the uniform models will tend to overestimate production, whereas in the presence of a deep chlorophyll maximum, the production will be underestimated [*Platt et al.*, 1988]. Therefore our result that the vertically uniform models in general give underestimates of production emphasises the importance of the contribution of the deep-chlorophyll maximum to water column production.

When the results were integrated to basin scale, differences between the spectral and nonspectral models were negligible. But one should not overlook that this is mainly a consequence of the choice of the values of k_c and K_w used

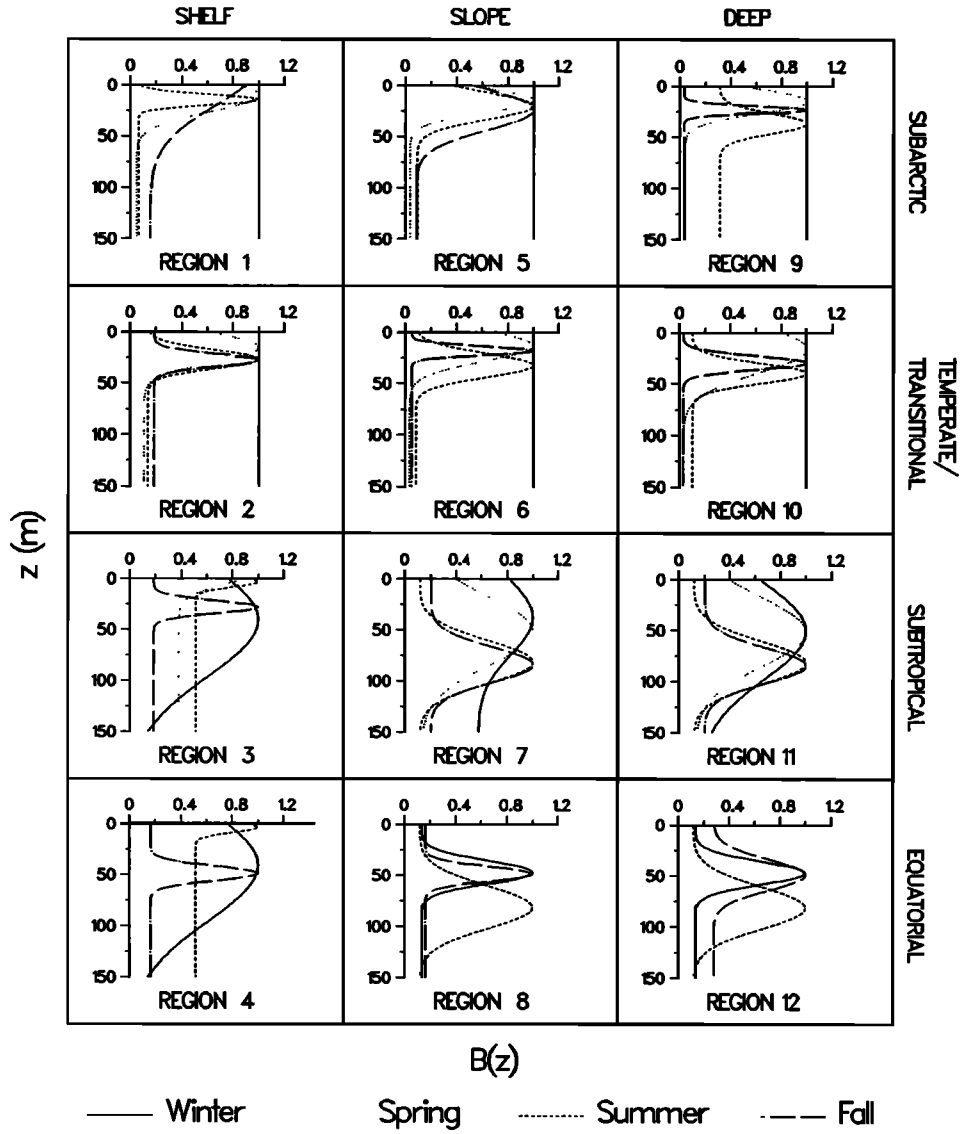

Fig. 1. The profiles of chlorophyll, for the 12 regions and the four seasons, used for the calculation of primary production in models 2 and 4. The profiles are drawn using the parameters listed in Table 3. For ease of comparison, the curves are normalized to unity at $z = z_m$. The spring profiles for the equatorial regions (regions 4, 8, and 12) are the same as the summer ones.

in the nonspectral models. These values were derived by linear regression of K against C computed for the photic zone (and for the photosynthetically active wavelength range) using a spectrally resolved optical model [see *Sathyendranath and Platt*, 1988]. In other words, these coefficients were "tuned" to match the spectral model as well as possible over a wide range in C. This tuning did not eliminate all the differences between spectral and nonspectral models for any given season or region (Figure 2), since the underlying relation between K and C is nonlinear [*Sathyendranath et al.*, 1989]. Residuals about the linear regression would be preferentially negative or positive in different parts of the range of C and would tend to compensate each other during integration over large-scale, heterogeneous, pigment fields. This result suggests that, with a more complete tuning of the parameters of the nonspectral model (different sets of parameters for different ranges of C), it should be possible to extend the applicability of the nonspectral models, with a corresponding economy of computing time [see also *Platt and Sathyendranath*, 1991].

Sensitivity to the Biomass Algorithm

In all the model calculations discussed so far, the biomass fields were derived using the method of *Sathyendranath and Platt* [1989*b*], rather than using the NASA algorithms, which form the conventional standard. This is because an analytical model is essential to investigate the consequences of nonuniformity in vertical structure. We used the same biomass algorithm for the uniform biomass models (models 1 and 3), for the sake of consistency (for evaluation of the effect of vertical structure on estimated production, it was important that the conclusions should not be obscured by a switch in biomass algorithm between uniform and nonuniform cases).

We have pointed out [*Sathyendranath and Platt*, 1989*b*]

TABLE 4. Parameters of the Photosynthesis-Light Curve for the 12 Regions of the Atlantic in Four Seasons

Region	P_m^B	α^B	N
	Winter		
1	1.49	0.057	1
2	3.68 (35)	0.157 (38)	14
3	2.64	0.053	1
4[a]			
5	1.58 (39)	0.073 (31)	6
6	1.80	0.127	1
7	3.55 (49)	0.078 (46)	5
8[a]			
9	2.63 (24)	0.098 (21)	9
10	2.97	0.105	1
11	4.80 (39)	0.165 (89)	5
12[b]			
	Spring		
1	1.42	0.052	1
2	3.01 (34)	0.087 (73)	38
3[c]			
4[d]			
5	1.94 (9)	0.056 (18)	6
6	1.93 (32)	0.045 (19)	3
7[e]			
8[d]			
9	2.55 (39)	0.113 (01)	2
10	2.69 (47)	0.064 (44)	7
11	1.87 (50)	0.127 (79)	2
12[f]			
	Summer		
1	2.95 (59)	0.064 (32)	8
2	5.10 (73)	0.140 (121)	58
3[g]			
4[d]			
5	2.56 (111)	0.083 (68)	11
6	4.29 (57)	0.054 (55)	19
7	7.17	0.031	1
8[d]			
9	2.42 (37)	0.062 (38)	6
10	5.18 (49)	0.046 (51)	6
11	4.11 (54)	0.035 (48)	4
12[f]			
	Fall		
1	1.75 (40)	0.057 (26)	6
2	5.22 (69)	0.149 (55)	17
3[h]			
4[a]			
5	1.39 (19)	0.047 (27)	8
6	1.33 (12)	0.039 (15)	2
7[i]			
8[a]			
9	1.63 (19)	0.057 (33)	4
10	1.44	0.035	1
11	5.02 (20)	0.049 (20)	2
12[b]			

For each parameter, the entry includes the mean over N observations, followed by the coefficient of variation (%) in parentheses. The parameter P_m^B is in mgC (mg Chl)$^{-1}$ h^{-1} and the parameter α^B is in mgC (mg Chl)$^{-1}$ (Wm^{-2})$^{-1}$ h^{-1}.

[a]No data: used region 7 (winter) data.
[b]No data: used region 11 (winter) data.
[c]No data: used region 2 (spring) data.
[d]No data: used region 7 (summer) data.
[e]No data: used region 6 (spring) data.
[f]No data: used region 11 (summer) data.
[g]No data: used region 2 (summer) data.
[h]No data: used region 2 (fall) data.
[i]No data: used region 6 (fall) data.

that some differences do exist between the analytical models of ocean color that are available now and the empirical algorithms for biomass retrieval, such as the ones used by NASA. To evaluate the uncertainty in the production values arising from the uncertainty in the estimation of biomass, we also ran the vertically homogeneous models with biomass calculated according to the NASA algorithms. Except at very low biomass, the NASA algorithm yields lower biomass for a given blue-green ratio than the analytical algorithm [*Sathyendranath and Platt*, 1989*b*]. We therefore found that the NASA algorithm yielded production values consistently lower than those from our models 1 and 3. On average, these estimates are almost 50% lower than would be calculated using the biomass retrieval algorithm of *Sathyendranath and Platt* [1989*b*]. We are therefore led to conclude that one of the major sources of uncertainty in calculation of primary production from remotely sensed data lies in the choice of algorithm for biomass retrieval.

Correlation Between Primary Production and Satellite-Derived Biomass

For better or for worse, many workers interpret ocean-color-pigment fields as if they were maps of primary production. To examine the reliability of untransformed biomass fields as indices of primary production, we plotted the average production for each region for a given month (estimated using model 4), as a function of the average, satellite-derived estimates of biomass for the same block (Figure 3). In general, the correlation between biomass and production is very weak. It is better for the equatorial regions ($0.65 \leq r^2 \leq 0.89$) than for the higher latitudes, presumably because of the lower variability in the incoming solar radiation over an annual cycle in the tropics. At higher latitudes, the r^2 values are much smaller (0.55 for region 9 but less than 0.29 elsewhere).

Therefore one should not expect that the primary production field will be a simple linear mapping of the biomass field, especially outside the tropics. Our results do not support the indiscriminate use of biomass as a proxy for primary production.

Basin-Scale Annual Production

The mean monthly production for each region was multiplied by the area covered by that region and integrated over regions and over months to estimate the production over the whole basin (20°S to 70°N). The regional results for model 4 calculations are presented in Table 5: they yield a value of 11.7 Gt C yr^{-1} after summation for the whole basin. Of this, coastal production (depth $\leq$ 200 m, regions 1–4) accounts for 2.3 Gt C yr^{-1}. Since the NASA biomass algorithm leads to production values that are (on average) 50% lower than those calculated with the biomass model of *Sathyendranath and Platt* [1989*b*], we may conclude that the annual production for the study area lies within the range from 6 to 12 Gt C yr^{-1}. Narrowing down the range more would require, at least, further improvements to the algorithms for the estimation of the biomass field from remote sensing.

The figures for primary production derived from satellites may be compared with earlier estimates: *Berger* [1989] estimated the production of the whole Atlantic Ocean to be 6.0 Gt C yr^{-1} of which 1.7 Gt C yr^{-1} were attributed to coastal regions. The estimates of *Platt and Subba Rao*

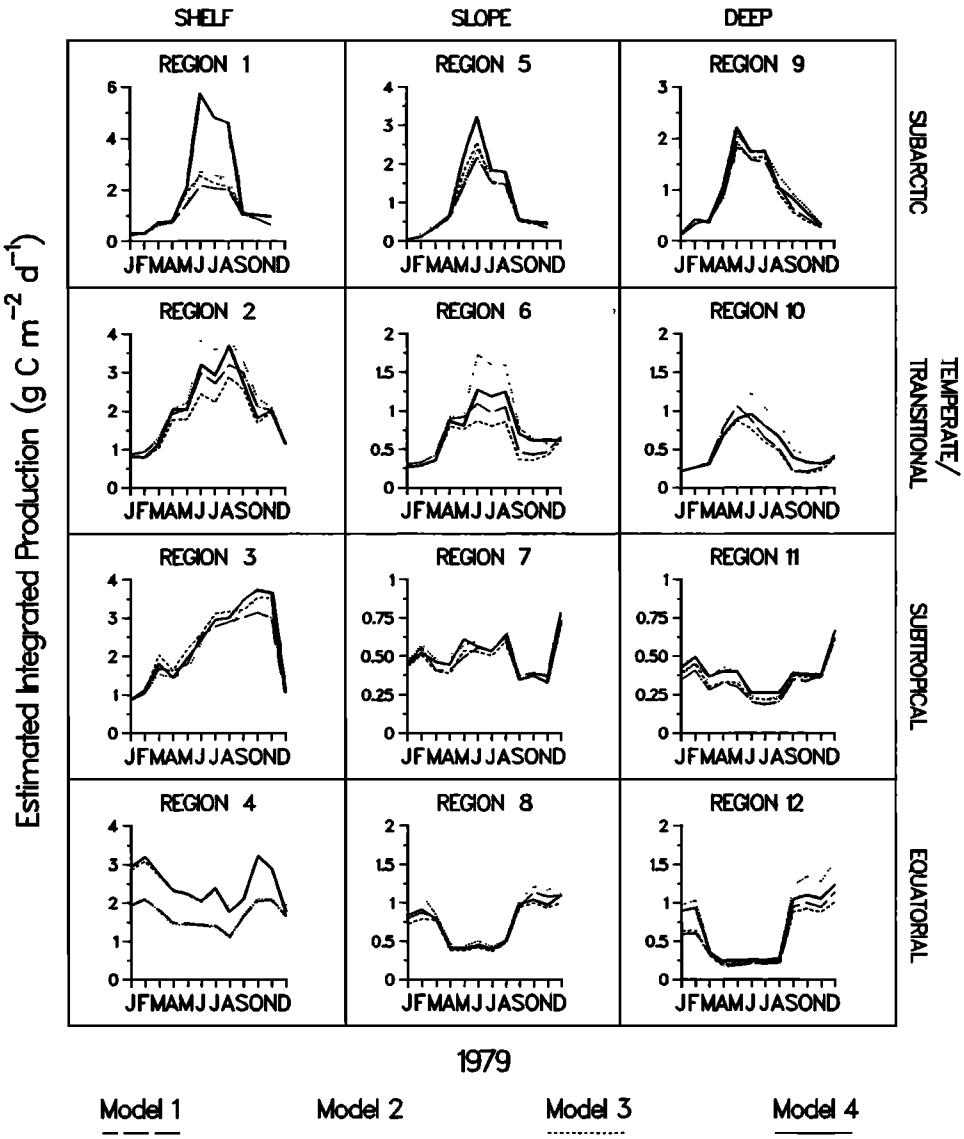

Fig. 2. The monthly production for the different regions, computed for all months of 1979, using the four different models.

[1975], which are now grossly out of date, were higher for the whole ocean (9.8 Gt C yr^{-1}) even though their estimate of production in the coastal regions of the Atlantic (1.3 Gt C yr^{-1}) was lower than that of *Berger* [1989]. The satellite estimates are therefore somewhat higher than the earlier estimates of primary production for the Atlantic based on sparsely distributed in situ measurements (especially considering that the present estimates do not include production south of 20°S, whereas the earlier estimates were for the whole of the Atlantic).

The following are among the ways that remote sensing might overestimate chlorophyll concentration and therefore the primary production:

1. In coastal regions, changes in ocean color due to suspended sediments or dissolved organic matter would be interpreted by the satellite as changes in chlorophyll concentration. The light transmittance models used in the paper are designed for open ocean waters ($C \leq 10$ mg m^{-3}), and in turbid coastal waters, these models are likely to overestimate the amount of light available at any given depth, which would again lead to overestimates in production. But, considering that coastal production (depth less than 200 m) accounts for less than 20% of the basin production, any error arising for this reason could not be a major source of overestimation at the basin scale.

2. The CZCS does not distinguish between chlorophyll and phaeopigments, which would lead to an overestimate of primary production if autotrophic activity were ascribed to photosynthetically incompetent pigments. In this instance we suspect that the errors, although potentially important, are at a minimum, since phaeopigments bleach rapidly in the presence of sunlight, and the satellite passes are made at local noon.

3. The high estimates from remote sensing may be due to the ability of the satellite to document in their entirety the otherwise inaccessible, spatially heterogeneous, pigment fields, thus taking into account the effect on integrated production of transient blooms in the open ocean, which are so frequently missed from in situ measurement techniques. We believe that this is the most likely explanation, and if we

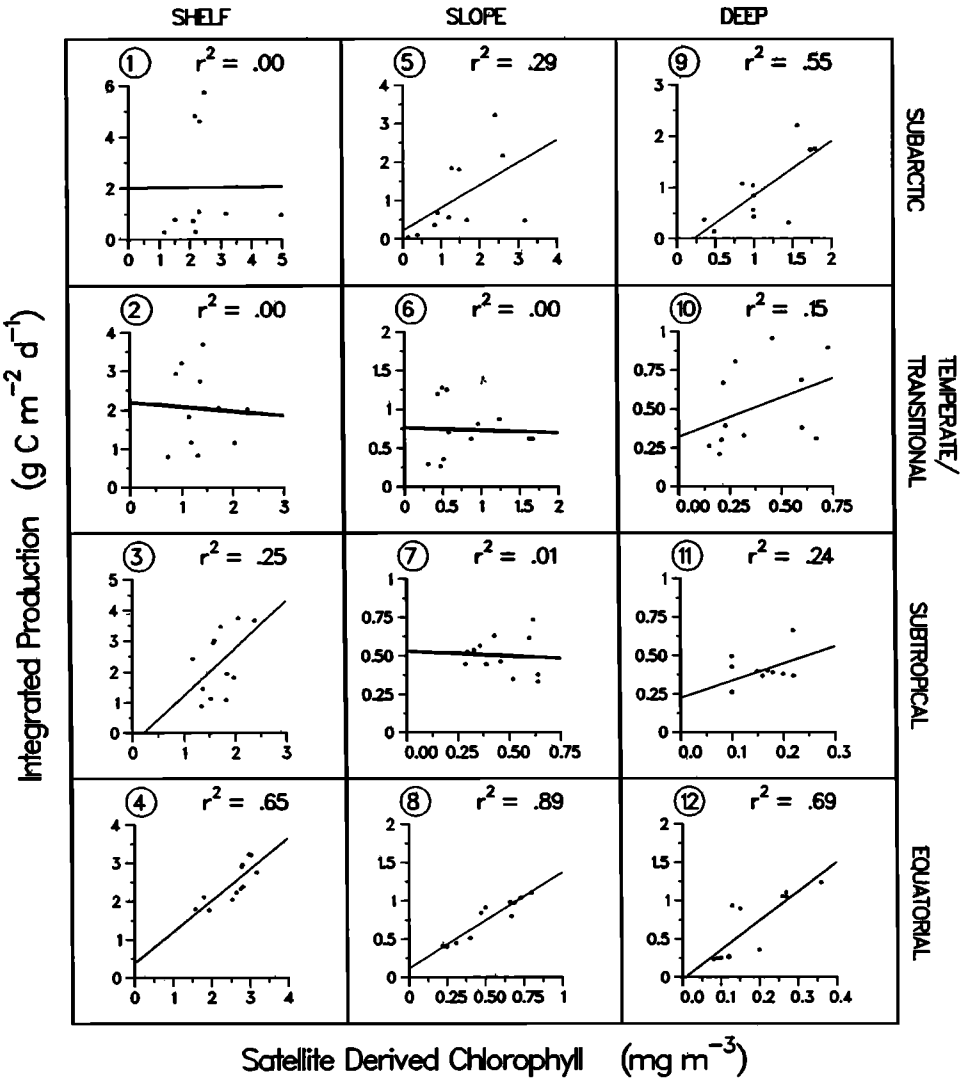

Fig. 3. The mean monthly production for each region plotted against the mean monthly (satellite-derived, NASA algorithm) biomass for that region. The straight lines are the best fits for each region. The coefficient of regression (r^2) is also given for each region.

are correct in this, it would be improper to refer to the high estimates as "overestimates" in the normal sense of the word.

Concluding Remarks

Concept of Biogeochemical Provinces

The archives used to characterize the different subregions were based on data collected for the most part (chlorophyll profiles) or entirely (photosynthesis-light parameters) by the Biological Oceanography Division of the Bedford Institute of Oceanography. They should therefore be internally consistent in the sense of their being relatively free from the effects of variations in sampling protocols and measurement procedures. Of course, the choice of boundaries to delineate the different subregions is, to some extent, arbitrary and subjective. We claim here to have made no more than a first step. Nevertheless, the partition we have used is preferable to treating the entire North Atlantic as a single, invariant unit with respect to the photosynthesis-light parameters and the

TABLE 5. Annual Primary Production Calculated for Each of the 12 Regions Using Model 4 With the Biomass Algorithm of *Sathyendranath and Platt* [1989*b*] and the Surface Area of Each Region

		Annual Primary Production	
Region	Area, 10^6 km^2	Grams Carbon per Square Meter per Year	Gigatons Carbon per Year
1	0.78	555	0.44
2	0.92	744	0.68
3	0.83	849	0.71
4	0.44	981	0.44
5	2.5	357	0.87
6	0.93	271	0.25
7	2.6	181	0.47
8	0.7	297	0.21
9	3.1	319	0.99
10	5.4	189	1.0
11	23	139	3.2
12	11	230	2.5

vertical structure parameters, since it is clear from Tables 3 and 4 that they differ substantially between seasons and regions. The utility of the concept of biogeochemical provinces will increase as more information accumulates on the variation of the parameters in the field.

Comparison Between Models

The significant errors incurred by ignoring the spectral structure of the irradiance field and the vertical structure of the water column justify the extra effort required to use a model complex enough to take them into account. The effects of wavelength and profile structure have been discussed previously [*Platt et al.*, 1988; *Sathyendranath et al.*, 1989] in a context where parameters were allowed to vary over the ranges of conceivable values. In the calculations discussed here, parameters are set at the best estimates of their values for a given application. The differences produced by the various algorithms are representative of the differences that may be expected in practical trials. There are circumstances in which the differences between models become negligible, but it would be unwise to assume that this would always be the case.

Comparison between biomass models indicates that possible error in biomass estimation is one of the major sources of uncertainty in the production estimates. This points to a clear need for further research, both theoretical and empirical, into the algorithms for biomass estimation from satellites. This is important particularly in view of the second generation of ocean color sensors planned for the future, such as SeaWiFS and MODIS, which will have better spectral and radiometric resolution than the CZCS and therefore more scope for improvements in retrieval techniques.

REMOTE SENSING FOR CALCULATION OF BASIN-SCALE PRIMARY PRODUCTION

Using the protocol proposed by *Platt and Sathyendranath* [1988], we have presented a calculation of the annual primary production at the basin scale for the North Atlantic Ocean. We expect that the estimate of annual production will be refined continuously as more information becomes available on the regional distribution of the parameters of vertical pigment structure and of photosynthetic performance, and as remote-sensing technology is improved. In addition to the anticipated improvements in the biomass retrieval algorithms with the advent of the next generation of ocean color sensors, techniques for estimating photosynthetically active radiation at the sea surface show promise of significant improvement (J. K. B. Bishop and W. B. Rossow, Spatial and temporal variability of global surface solar irradiance, submitted to *Journal of Geophysical Research*, 1991).

The delineation of the biogeographic, or biogeochemical, provinces is crude in our treatment. We have taken their boundaries to be parallel to the equator and constant in time. The next level of refinement would be a more closely justified partition of the provinces, allowing the boundaries to vary with seasons where necessary. We believe that the most useful tool for working toward this goal will be the biomass fields themselves, in particular their features that repeat from year to year.

Despite our qualification that the figure presented here for annual primary production should be regarded as an interim one, we remain convinced that we have identified [*Platt et al.*, 1988; *Sathyendranath and Platt*, 1988; *Platt and Sathyendranath*, 1988; *Sathyendranath and Platt*, 1989*a*, *b*; *Sathyendranath et al.*, 1989; *Platt et al.*, 1990; *Platt and Sathyendranath*, 1991] the elements that must be studied if the primary production estimates are to be improved. Of these, the most important are the vertical structure of the chlorophyll profile and of the photosynthesis parameters and how they are distributed at regional space scales and seasonal time scales. It will be essential to know about these regardless of the method chosen to calculate primary production.

Annual primary production for the Atlantic, within the interval 70°N and 20°S, evaluated using the parameters of the biogeographic provinces and the monthly fields of biomass derived from satellite data, is about 9 (± 3) Gt C yr^{-1}. This is somewhat higher than earlier estimates for the region, which were made without the benefit of remotely sensed data on the biomass fields.

We are fully aware that some people may be unwilling to accept a figure for primary production based on remote sensing if it diverges from those made using only observations from ships. Scepticism could arise, among other reasons, from the recognition that the biomass results themselves carry a substantial error of estimation, that biomass deeper in the photic zone is progressively less visible to the satellite, and from the procedure used to convert biomass into production.

We believe, however, that the remote-sensing method for large-scale estimates of primary production is intrinsically superior to any method based on ship observations alone, because it is the most complete method available. The remote-sensing approach to primary production implies supplementing the ship observations with satellite data, and not replacing the ship observations with remotely sensed data. The remotely sensed information adds to the information already available from in situ observations. No information is discarded. All the data are used. The ship observations, collectively, serve to reinforce and consolidate the partition of the ocean into subregions for orderly extension of the local algorithm into a tool useful at the basin scale.

Moreover, the remote-sensing method adds information that cannot be found by any other means. Consider that primary production is calculated as the product of a biomass and a biomass-specific rate $P = B \times P^B$. Now consider that B has a dynamic range of more than 10^4 over regions and seasons. Clearly, it is essential to have information on B, as well as on P^B, if our large-scale estimates of primary production are to be reliable. Given that remote sensing provides information about the spatial distribution of phytoplankton on scales inaccessible for in situ observations, basin- or global-scale estimates of ocean primary production that exploit satellite data are an improvement over methods that do not.

Satellite data on ocean color have revolutionized our knowledge of the chlorophyll distribution in the ocean. Remote sensing has revealed an intense variability of the autotrophic biomass in time and space, even in the open ocean, that leads us to appreciate the total inadequacy of the former method for estimation of primary production at the basin scale: the compilation of sparsely sampled, in situ data

collected in different years with no systematic plan in respect of season or location. Even for an estimate of the long-term average of annual primary production, this would be an inferior approach at best. For study of interannual changes in ocean production, for example, in response to climate change, remote sensing offers the only possible approach.

The remote-sensing method for estimation of primary production at large horizontal scale is the only method that makes use of all the available information. It is based on the first principles of plant physiology. It exploits the accumulated knowledge on the structure and function of the ocean ecosystem at regional and seasonal scales. It uses remote sensing only to supply vital information on the biomass field and its variability, which is known to be considerable. Such information is unobtainable by any other method but is essential if the calculation is to take into account the episodic blooms which are now known to be a characteristic feature everywhere in the ocean. We therefore take the view that for calculation of primary production at the ocean basin scale, the remote-sensing method is the method of choice.

Acknowledgments. The work presented in this paper was supported by the Office of Naval Research, the National Aeronautics and Space Administration, and the Department of Fisheries and Oceans, Canada. Additional support was provided by the Natural Sciences and Engineering Research Council through Operating Grants to S.S. and TP. We thank three anonymous referees for constructive comments on the manuscript. We thank J. E. O'Reilly and A. Herbland for sending us their detailed data.

REFERENCES

Berger, W. H., Global maps of ocean productivity, in *Productivity of the Ocean: Present and Past*, edited by W. H. Berger, V. S. Smetacek, and G. Wefer, pp. 429–455, John Wiley, New York, 1989.

Bermuda Biological Station, Physical, chemical and biological observations in the Sargasso Sea off Bermuda, 1957–1960: The plankton ecology, related chemistry and hydrography of the Sargasso Sea, final report: May 1, 1959–August 31, 1960, part 3, St. George's West, Bermuda, U.S. At. Energy Comm. contract AT (30-1)-2078, p. 80, 1960.

Bird, R. E., A simple, solar spectral model for direct-normal and diffuse horizontal irradiance. *Solar Energy*, *32*, 461–471, 1984.

Denman, K., B. Irwin, and T. Platt, Phytoplankton productivity experiments and nutrient measurements at the edge of the Nova Scotia continental shelf between June 28 and July 12, 1976, *Data Rep. Fish. Mar. Serv.*, *708*, xiii + 205 pp., 1977.

Gordon, H. R., and D. K. Clark, Remote sensing optical properties of a stratified ocean: an improved interpretation, *Appl. Opt.*, *19*, 3428–3430, 1980.

Hahn, C. J., S. G. Warren, J. London, R. L. Jenne, and R. M. Chervin, Climatological data for clouds over the globe from surface observations, *Rep. NDP-026*, Carbon Dioxide Inf. Cent., Oak Ridge, Tenn., 1987.

Irwin, B., and T. Platt, Phytoplankton productivity and nutrient measurements at the edge of the continental shelf off Nova Scotia between June 3 and June 6, 1978, *Can. Data Rep. Fish. Aquat. Sci.*, *174*, v + 50 pp., 1979.

Irwin, B., T. Platt, A. D. Jassby, and D. V. Subba Rao, The relationship between light intensity and photosynthesis by phytoplankton. Results of experiments at three stations in the coastal waters of Nova Scotia, *Data Rep. Fish. Mar. Serv.*, *595*, xi + 205 pp., 1975.

Irwin, B., P. Evans, and T. Platt, Phytoplankton productivity experiments and nutrient measurements in the Labrador Sea from 15 October to 31 October 1977, *Data Rep. Fish. Mar. Serv.*, *83*, iv + 40 pp., 1978*a*.

Irwin, B., P. Evans, and T. Platt, Phytoplankton productivity experiments and nutrient measurements in the Labrador Sea, from 11 February to 28 February 1978, *Data Rep. Fish. Mar. Serv.*, *114*, iv + 38 pp., 1978*b*.

Irwin, B., W. G. Harrison, K. L. Denman, and T. Platt, Phytoplankton productivity and nutrient measurements at the edge of the continental shelf off Nova Scotia between April 28 and May 11, 1977, *Data Rep. Fish. Mar. Serv.*, *62*, iv + 90 pp., 1978*c*.

Irwin, B., M. Hodgson, P. Dickie, and T. Platt, Phytoplankton productivity experiments in Baffin Bay and adjacent inlets from 22 August to 18 September 1977, *Data Rep. Fish. Mar. Serv.*, *82*, iv + 52 pp., 1978*d*.

Irwin, B., W. G. Harrison, C. L. Gallegos, and T. Platt, Phytoplankton productivity experiments and nutrient measurements in the Labrador Sea, Davis Strait, Baffin Bay and Lancaster Sound from 26 August to 14 September 1978, *Can Data Rep. Fish. Aquat. Sci.*, *213*, iv + 103 pp., 1980.

Irwin, B., T. Platt, W. G. Harrison, C. L. Gallegos, and P. Lindley, Phytoplankton productivity experiments and nutrient measurements in Ungava Bay N.W.T. from August 1 to September 3, 1979, *Can. Data Rep. Fish. Aquat. Sci.*, *287*, iv + 208 pp., 1982.

Irwin, B., C. Caverhill, D. V. Subba Rao, C. Carver, and T. Platt, Primary productivity measurements in the chlorophyll maximum in the vicinity of the Mid-Atlantic Ridge, west of the Azores, from 8 July to 25 July, 1982, *Can. Data Rep. Fish. Aquat. Sci.*, *402*, iv + 84 pp., 1983*a*.

Irwin, B., L. Harris, P. Dickie, P. Lindley, and T. Platt, Phytoplankton productivity in the eastern Canadian Arctic during July and August 1980, *Can. Data Rep. Fish. Aquat. Sci.*, *386*, iv + 157 pp., 1983*b*.

Irwin, B., L. Harris, M. Hodgson, E. Horne, and T. Platt, Primary productivity and nutrient measurements in Northern Foxe Basin, N.W.T. from 27 August to 7 September 1981, *Can. Data Rep. Fish. Aquat. Sci.*, *385*, iv + 40 pp., 1983*c*.

Irwin, B., P. Lindley, C. L. Gallegos, and T. Platt, Phytoplankton productivity experiments on the Scotian Shelf from April 18 to May 2, 1979, *Can. Data Rep. Fish. Aquat. Sci.*, *384*, iv + 118 pp., 1983*d*.

Irwin, B., T. Platt, P. Lindley, M. J. Fasham, and K. Jones, Phytoplankton productivity in the vicinity of a front, S.W. of the Azores during May 1981, *Can. Data Rep. Fish. Aquat. Sci.*, *400*, iv + 101 pp., 1983*e*.

Irwin, B., C. Caverhill, W. G. Harrison, and T. Platt, Primary production in the Sargasso Sea northeast of Bermuda in April 1983, *Can. Data Rep. Fish. Aquat. Sci.*, *550*, iv + 83 pp., 1985*a*.

Irwin, B., T. Platt, and C. Caverhill, Primary production and other related measurements in the eastern Canadian Arctic during the summer of 1983, *Can. Data Rep. Fish. Aquat. Sci.*, *510*, iv + 143 pp., 1985*b*.

Irwin, B., C. Caverhill, P. Dickie, E. Horne, and T. Platt, Primary productivity on the Labrador Shelf during June and July 1984, *Can. Data Rep. Fish. Aquat. Sci.*, *577*, iv + 162 pp., 1986*a*.

Irwin, B., C. Caverhill, and T. Platt, Primary production on the Grand Banks of Newfoundland in April 1984, *Can. Data Rep. Fish. Aquat. Sci.*, *579*, iv + 49 pp., 1986*b*.

Irwin, B., C. Caverhill, J. Anning, D. Mossman, and T. Platt, Primary production on Georges Bank and in the northern Sargasso Sea in July and August 1985, *Can. Data Rep. Fish. Aquat. Sci.*, *670*, iv + 362 pp., 1987*a*.

Irwin, B., C. Caverhill, J. Anning, and T. Platt, Primary production and related measurements at a fixed station in the Caribbean Sea in December 1984, *Can. Data Rep. Fish. Aquat. Sci.*, *671*, iv + 161 pp., 1987*b*.

Irwin, B., C. Caverhill, J. Anning, D. Mossman, and T. Platt, Carbon and oxygen primary production in Bedford Basin, Nova Scotia from March to June 1985, *Can. Data Rep. Fish. Aquat. Sci.*, *686*, iv + 135 pp., 1988*a*.

Irwin, B., C. Caverhill, T. Platt, I. Joint, and M. Fasham, Primary production in the Celtic Sea in May and June 1986, *Can. Data Rep. Fish. Aquat. Sci.*, *718*, iv + 241 pp., 1988*b*.

Irwin, B., P. Dickie, M. Hodgson, and T. Platt, Primary production and nutrients on the Labrador Shelf, in Hudson Strait and Hudson Bay in August and September 1982, *Can. Data Rep. Fish. Aquat. Sci.*, *692*, iv + 139 pp., 1988*c*.

Irwin, B., W. G. Harrison, J. Anning, C. Caverhill, P. Dickie, and T. Platt, Phytoplankton production and distribution on the Grand Banks of Newfoundland in September 1985, *Can. Data Rep. Fish. Aquat. Sci.*, *691*, iv + 82 pp., 1988*d*.

Irwin, B., C. Caverhill, J. Anning, A. Macdonald, M. Hodgson, E. P. W. Horne, and T. Platt, Productivity localized around seamounts in the Atlantic (PLASMA) during June and July 1987, *Can. Data Rep. Fish. Aquat. Sci., 732*, iv + 227 pp., 1989*a*.

Irwin, B., C. Caverhill, D. Mossman, J. Anning, E. Horne, and T. Platt, Primary productivity on the Labrador shelf during July 1985, *Can. Data Rep. Fish. Aquat. Sci., 760*, iv + 119 pp., 1989*b*.

Irwin, B., J. Anning, C. Caverhill, M. Hodgson, A. Macdonald, and T. Platt, Primary production in the northern Sargasso Sea in September 1988, *Can. Data Rep. Fish. Aquat. Sci., 798*, iv + 93 pp., 1990*a*.

Irwin, B., J. Anning, C. Caverhill, A. Macdonald, and T. Platt, Primary production on Georges Bank—August 1988. *Can. Data Rep. Fish. Aquat. Sci., 785*, iv + 197 pp., 1990*b*.

Irwin, B., J. Anning, C. Caverhill, and T. Platt, Primary production on the Labrador Shelf and in the Strait of Belle Isle in May 1988. *Can. Data Rep. Fish. Aquat. Sci., 784*, iv + 96 pp., 1990*c*.

Irwin, B., J. Anning, J. Goes, M. Hodgson, E. Horne, A. Macdonald, and T. Platt, The North Atlantic Pilot Project. April 20-May 20 1989. *Can. Data Rep. Fish. Aquat. Sci.*, in press, 1991.

Levitus, S., Climatological atlas of the world ocean, *NOAA Prof. Pap. 13*, xv + 173 pp., U.S. Govt. Print. Off., Washington, D.C., 1982.

Mueller, J. L., and R. E. Lange, Bio-optical provinces of the Northeast Pacific Ocean: A provisional analysis, *Limnol. Oceanogr., 34*, 1572–1586, 1989.

O'Reilly, J. E., and D. A. Busch, Phytoplankton primary production on the northwestern Atlantic shelf. *P. V. Reun. Cons. Int. Explor. Mer, 183*, 255–268, 1984.

O'Reilly, J. E., C. Evans-Zetlin, and D. A. Busch, Primary production, in *Georges Bank*, edited by R. Backus, pp. 220–233, M.I.T. Press, Cambridge, Mass., 1987.

Paltridge, G. W., and C. M. R. Platt, *Radiative Processes in Meteorology and Climatology*, 318 pp., Elsevier Scientific, New York, 1976.

Platt, T., Primary production of the ocean water column as a function of surface light intensity: Algorithms for remote sensing, *Deep Sea Res., 33*, 149–163, 1986.

Platt, T., and S. Sathyendranath, Oceanic primary production: Estimation by remote sensing at local and regional scales, *Science, 241*, 1613–1620, 1988.

Platt, T., and S. Sathyendranath, Biological production models as elements of coupled, atmosphere-ocean models for climate research, *J. Geophys. Res., 96*, 2585–2592, 1991.

Platt, T., and D. V. Subba Rao, Primary production of marine microphytes, in *Photosynthesis and Productivity in Different Environments*, vol. 3, edited by J. P. Cooper, pp. 249–280, Cambridge University Press, New York, 1975.

Platt, T., C. L. Gallegos, and W. G. Harrison, Photoinhibition of photosynthesis in natural assemblages of marine phytoplankton, *J. Mar. Res., 38*, 687–701, 1980.

Platt, T., S. Sathyendranath, C. M. Caverhill, and M. R. Lewis, Ocean primary production and available light: Further algorithms for remote sensing, *Deep Sea Res., 35*, 855–879, 1988.

Platt, T., S. Sathyendranath, and P. Ravindran, Primary production by phytoplankton: Analytic solutions for daily rates per unit area of water surface, *Proc. R. Soc. London, Ser. B, 241*, 101–111, 1990.

Sathyendranath, S., and T. Platt, The spectral irradiance field at the surface and in the interior of the ocean: A model for applications in oceanography and remote sensing, *J. Geophys. Res., 93*, 9270–9280, 1988.

Sathyendranath, S., and T. Platt, Computation of aquatic primary production: Extended formalism to include effect of angular and spectral distribution of light, *Limnol. Oceanogr., 34*, 188–198, 1989*a*.

Sathyendranath, S., and T. Platt, Remote sensing of ocean chlorophyll: Consequence of non-uniform pigment profile, *Appl. Opt., 28*, 490–495, 1989*b*.

Sathyendranath, S., T. Platt, C. M. Caverhill, R. E. Warnock, and M. R. Lewis, Remote sensing of oceanic primary production: Computations using a spectral model, *Deep Sea Res., 36*, 431–453, 1989.

Smith, E. L., Photosynthesis in relation to light and carbon dioxide, *Proc. Natl. Acad. Sci. U.S.A., 22*, 504–511, 1936.

Woods Hole Oceanographic Institution, Physical, chemical and biological observations in the Sargasso Sea off Bermuda, 1960–1963: Progress report submitted to the U.S. Atomic Energy Commission under contract AT (30-1)-3140, Reference 64-8, Appendix II, p. 75, Woods Hole, Mass., 1964.

C. Caverhill and T. Platt, Biological Oceanography Division, Bedford Institute of Oceanography, Box 1006, Dartmouth, Nova Scotia, Canada, B2Y 4A2.

S. Sathyendranath, Department of Oceanography, Dalhousie University, Halifax, Nova Scotia, Canada, B3H 4J1.

(Received January 7, 1991;
accepted March 28, 1991.)